Hindawi
Advances in Civil Engineering
Volume 2022, Article ID 2191315, 15 pages
https://doi.org/10.1155/2022/2191315

Research Article

A Multiplex Conversion of a Historical Cinema

Alessio Cascardi,[1] **Salvatore Verre**,[2] **Alessandra Sportillo**,[3] **and Gaetano Giorgio**[4]

[1]*ITC-CNR National Council of Research, Sede Secondaria di Bari–70124, Italy*
[2]*University of Calabria, Rende–87036, Italy*
[3]*University of Salento, Lecce–73100, Italy*
[4]*Studio "Giorgio&Partners", Toritto–70020, Italy*

Correspondence should be addressed to Alessio Cascardi; alessio.cascardi@itc.cnr.it

Received 10 June 2021; Revised 25 January 2022; Accepted 24 February 2022; Published 16 March 2022

Academic Editor: Andreas Lampropoulos

The cultural building Heritage is a valuable trace of the past social life in a city. One peculiar typology of building is the theatre or, more recently, the cinema. Within this indoor space, the community of people actively live an emotional feeling over the time causing memories linked to not only the show itself, but also to the place. Furthermore, cinemas are often located in city centers where buildings are historical-oriented form the architectural point of view and, for this reason, their added-value needs to be recognized. Currently, the modernization and the improvement of old cinemas is becoming an interesting topic in the field of civil engineering. In order to empathize this aspect, the structural strengthening for a multiplex conversion of an historical cinema is herein reported. The studied structure required a seismic joint (separating the masonry to the reinforced concrete structural bodies) and a severe strengthening of a very long span beam due to a relevant overloading (in seismic loads combination) caused by the new architectonical project. The numerical simulations demonstrated the validity of two bending strengthening systems (i.e. Fiber Reinforced Polymer-plate and *Beton Plaquè*) in terms of both load bearing capacity and maximum deflection. This overview is a part of a larger study in the way of a global structural interventions which will also involve the masonry members.

1. Introduction

Currently, the construction business is more oriented on the conservation, strengthening and regeneration of existing buildings instead of new constructions. This aspect is particularly felt in the case of the social and cultural building Heritage. In fact, the public buildings often cannot be erected in new places since the serviceability and the accessibility are linked aspects. Thus, the structures located in city centers need to be focused. An example is the cinema/theatre. In Italy, there are many cases of old cinemas which are now abandoned because not able to cover the modern demand from the public anymore. In fact, the structures are often ancient from the normative point of view (e.g. in seismic capacity) and the projection rooms are inadequate in terms of both the technology and the dimensions/capacity. In order to reuse this important Heritage, the seismic update is mandatory while a more functional architectonic project is attended. Therefore, the structural analysis involves many action steps: geometrical and structural survey (diagnostic), global analysis *ante-operam*, choice of the strengthening interventions, design, global analysis *post-operam* and monitoring according to the ISCARSAH's Recommendations and many other cases study, [1–6].

In the past decades, there were many examples of cinema reconversions or updating, [7]. For example, in Italy many cinemas were converted into multiplexes in the 2000s following major renovations: the *Cinema Massimo* in Turin, the *Cinema Orfeo* in Milan and the *Cinema Massimo* in Lecce. In particular, the *Cinema Massimo* in Turin was built in the 1930s and had only one auditorium with 1000 seats capacity. It was re-designed a few years later due to the bombings of 1942 (II World War). Following the crisis of the 1980s, the cinema was closed and re-opened in 2001 after a renovation. Currently, the *Cinema Massimo* is arranged into three projection rooms: one with 453 seats and two with 147 seats.

The *Cinema Orfeo* in Milan was opened in 1936 and damaged in 1943 by bombing (again during the II World War). It had a single 2500-seats auditorium and was considered for many years the largest cinema in Milan and among the largest in Europe. In 2004, following a renovation, the cinema was converted into a multiplex with three new rooms: one with 720 seats and two with 290 seats. Finally, the construction of the *Cinema Massimo* in Lecce began in 1939, but it was interrupted during the II World War, only to be resumed later. At the beginning, it had only one theatre with 700 seats. Towards the end of the 1990s, renovation work occurred and the cinema was converted into a multiplex with five auditoriums: one with 675 seats and an opening roof, two auditoriums with 150 seats, one with 144 seats and the last one with 130 seats.

In the present paper, the case-study of the ex "*Supercinema*" in*Trani* is reported and discussed. The study is new and the findings are original. The peculiarities of the selected building are recognizable in its mixed-structure (almost half masonry and half reinforced concrete made) and the presence of a very long-span beam which is the target of a *Finite Element* (FE) analysis herein performed.

2. Descriptions of the Building

The so called *Supercinema* is placed in the center of the *Trani*, a quite small city in the south of Italy (see Figure 1(a)). The structure consists in two adjacent bodies of a different construction system: masonry and reinforced concrete (RC) as illustrated in Figure 1(b). An intermediate floor makes the conjunction of the two bodies.

Passing throughout the main entrance, according to the original functional conception (Figure 2(a)), the building has a load-bearing masonry structure, consisting of two elevations above the ground. At the ground floor, the one used for the cinema/theatre purpose, an entrance hall is dominating the space; while a small projection room (Figure 2(b)) is on the left opposite to the offices and the toilets. The roofs of the first level are barrel vaults, with a maximum height of 5.20 m. Before entering into the theatre, a short-lived of the transition area under the conjunction floor is found. It is a single-story area consisting of a connecting slab. Here, a corner bar is located (Figures 2(c) and 2(d)). The RC-building which houses the theatre consists of three floors above ground and one basement, all of them can be accessed by stairs located at the corners. On the ground floor there is the stage and the stalls, currently without seats, while on the first and second floors there are two galleries that will be converted into recreational areas (on the first floor) and three additional halls (on the second floor) as better shown in the next sections. When entering within the "core" of the theatre, a very long span beam, supported on octagonal cross section columns, dominate the structural behavior and the architectural view (Figure 2(e)). The mentioned span is about 14 m and, therefore, much longer than the others, which have an average length of 4.00 m. For this reason, a series of transversal beams were constructed in order to limit the potential mid-span deflection (Figures 2(f) and 2(g)). The other beams are supported by prismatic cross section columns (Figure 2(h)). The whole photos views are reported in Figure 2 in order to make the understanding of the building conceptual design cleaner and easier.

There were about two thousand seats, which are currently dismantled. The floor height of the stalls ranging between 6.00 m to 9.90 m, while the height of the galleries on the second and third floors is about 2.75 m. Instead, the height of the stage is 12.00 m.

2.1. Territorial Framework. *Trani* is located on the Adriatic coast, 45 km north from the capital city of Bari. Together with *Andria* and *Barletta*, it makes one of the six provincial capitals of the *Apulia* region. According to an ancient legend, the name *Trani* is linked to *Tyrrhenus*, son of the Greek mythological hero Diomedes, who founded the city in the 3rd century a.C. However, some modern scholars have established two different hypotheses regarding the origin of the name: the first is that *Trani* may be the shortened form of *Trajan* (a name that may have been given to the city in honor of the Roman Empire) and the second is that the name derives from the medieval term "*trana*", which indicated an inlet suitable for fishing: an inlet that currently corresponds to the city port. In urban terms, *Trani* is divided into three main areas:

(1) The historic center, surrounded by huge masonry walls by 1846, embellished by palaces and historical monuments, as well as, by narrow and winding streets. It is the most characteristic area of the city, close to the port and the cathedral.

(2) Nineteenth-century village, a wealthy and aristocratic area, characterized by villas and palaces of the period. The Supercinema falls within this area.

(3) A residential and modern area, which grew rapidly at the beginning of the 20th century due to the expansion of the city. It branches off beyond the 19th-century village, mainly to the south towards *Bisceglie* and from the 1950s also to the west towards *Andria* and *Corato*. There were no expansion northwards towards *Barletta* due to the presence of the industrial area.

2.2. Historical Background. The *Supercinema* was commissioned by Giuseppe Boccasini, who had returned to *Trani* after had success in America, Domenico Di Mango, foreman of the Aswan dam and an expert in reinforced concrete structure, Domenico Persano, a large landowner from Lecce, and Nicola Guacci, stationmaster, with his wife Lucia Laurora. The Figure 3(a) shows the principals of the *Supercinema* at the early-stage construction. The on-site activities began in 1934 under the supervision of the engineer Enrico Bovio and the inauguration took place the following year, arousing great amazement from the Trani public and numerous foreigners who flocked to the town to see a film in the area's first state-of-the-art cinema, even though it was the only cinema with about two thousand seats (see Figure 3(b)).

The theatre has undergone several modifications:

Figure 1: The SUPERCINEMA in Trani: (a) front view and (b) structure typologies individuation.

(i) in 1991 the renovation of the installations, the stage and the dressing rooms;

(ii) in 1991 the construction of a false ceiling;

(iii) in 1995 the general renovations and adaptations;

(iv) in 2002 the construction of a new hall to replace the second gallery and the conversion of an internal room into a projection room.

However, it has now been closed since 2008 and subjected to historical and architectural restrictions. Lastly, in April 2019, the removing of the asbestos roof was performed.

2.3. In-Situ Surveys. The accuracy of a structural strengthening design is based, above all, on the initial knowledge mining phase, by carrying out a preliminary test campaign that investigates the mechanical properties of the construction materials, the geometry, the state of decay, the level of damage, etc. According to Italian code NTC 2018 [8, 9], based on the quantity and the typology (destructive or not destructive) of the investigations carried out in the cognitive phases, a certain LC (*Level of Confidence*) is reached. The LC has three options: LC1, LC2 and LC3. As a congruence, a corresponding partial factor is identified, namely the CF (*Confidence Factors*), which can assume the value of 1.35, 1.2 and 1 respectively. The aspects that define the levels of confidence are: geometry of the structure, construction details, material properties, connections between the various elements and their presumed modes of collapse. The confidence factor is used for the reduction of the average values of the mechanical parameters from in-situ tests (e.g. strength of the materials) and must be understood as indicators of the level of detailing achieved. Concerning the herein reported case-study, only the RC building was investigated by performing non-destructive tests. Instruments used were the pacometer, the thermo-camera and the combined *SonReb* test. Therefore, the investigations were limited at that moment providing a LC1 and a FC = 1.35. More details of the diagnosis are reported in the following sections.

2.3.1. Pacometer. In the *Supercinema*, the pacometric tests were carried out on the beam with a 13.9 m span and on the 30×35 cm rectangular cross section columns near the exits on the opposite side of the platform. By referring to the beam (see Figure 4), the recordings revealed that the cross section has uniform concrete cover with 1–2 cm thickness, a total of 5Φ20 bottom longitudinal reinforcement rebars and Φ8/30 cm stirrups, although the span was not constant. The upper longitudinal reinforcement was assumed equal to 2Φ20 to be on the conservative side. On the other hand, the column (see Figure 5) figured out an almost uniform concrete cover with 1–2 cm thickness, a set of 3Φ20 longitudinal rebars per side and Φ8/35 cm arranged for transversal reinforcement.

2.3.2. SonReb. The in-situ compressive strength of the concrete can be influenced by numerous factors, such as carbonation, amount of internal reinforcing steel, as well as, their location and/or the aggregate size. It is well-known that the most accurate compressive strength estimation can be determined by combining different testing techniques. For example, the correlation of data from the *Schmidt hammer* and *ultrasonic tester* to the existing compressive strength

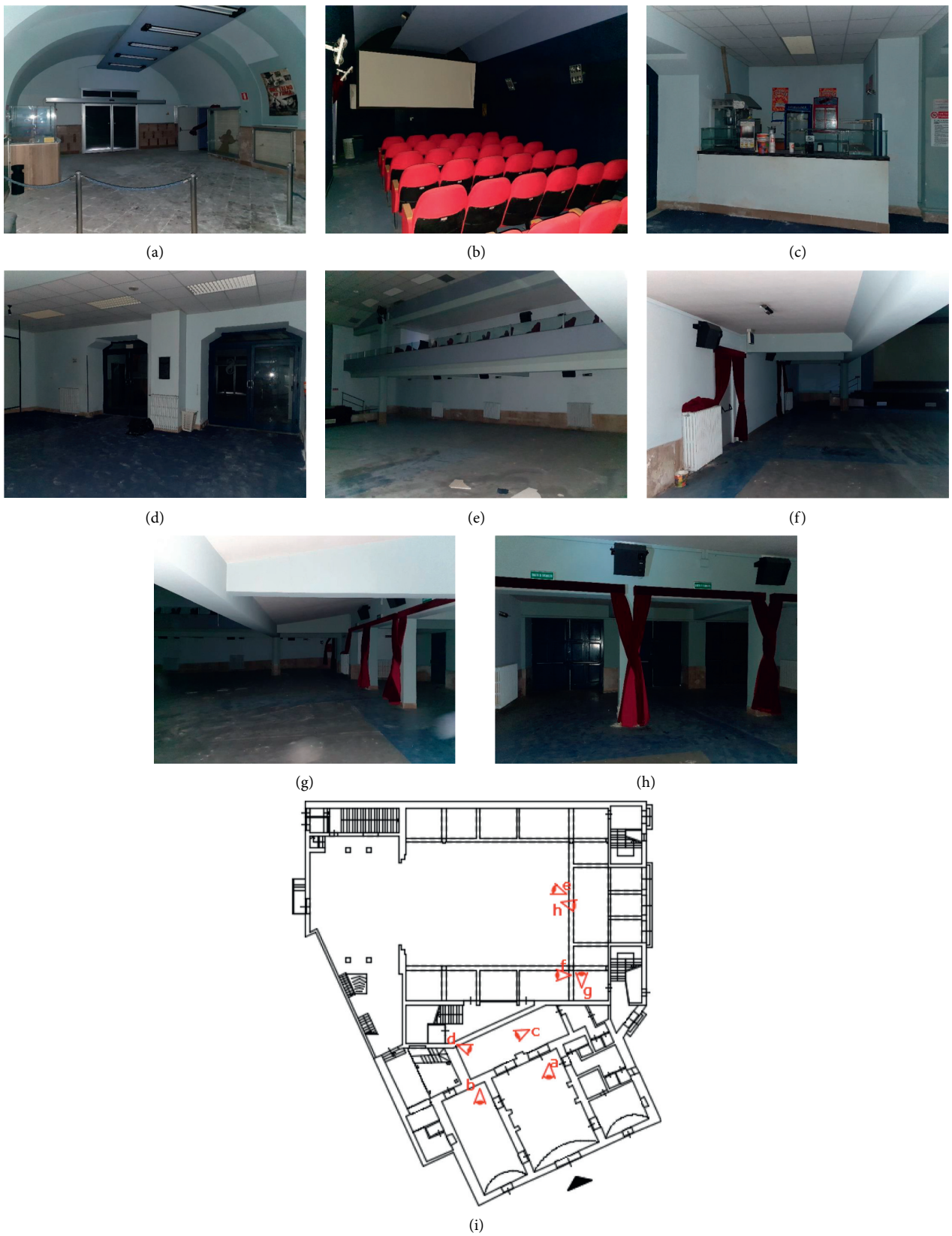

Figure 2: (a-h) inside photos and (i) plan with trigger points.

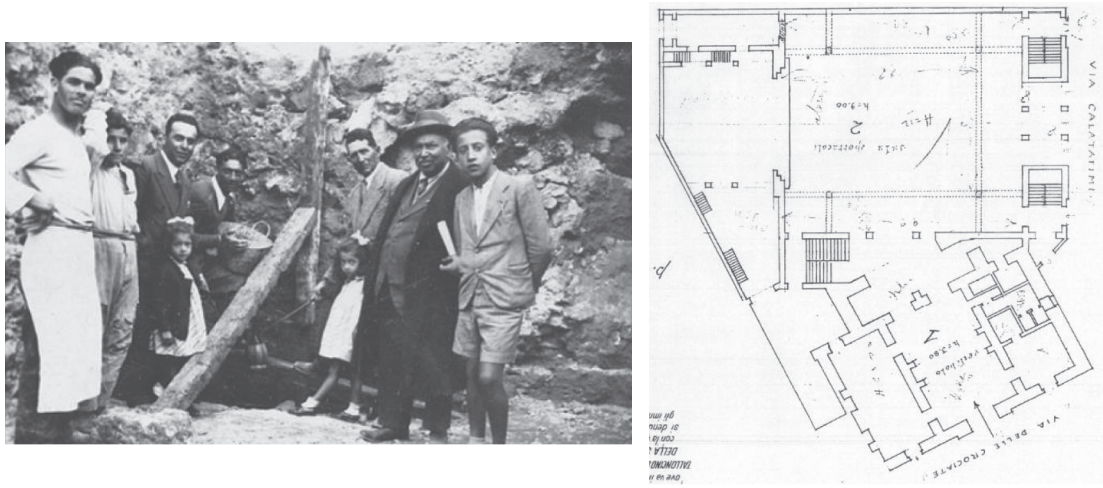

Figure 3: Historical photos: principals (a) and original structure design (b).

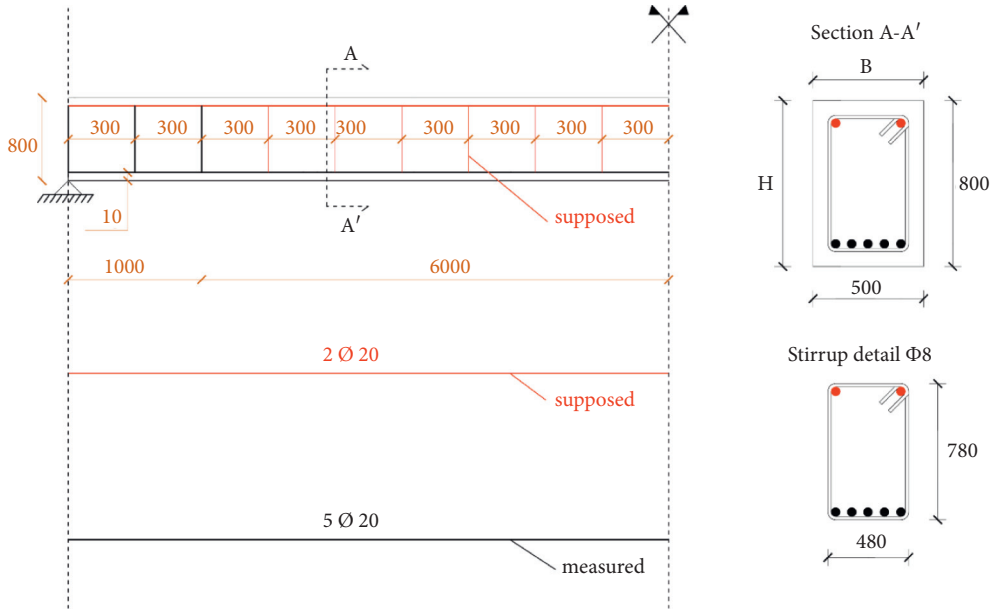

Figure 4: Identification of internal reinforcing bars of the very long span beam: cross section (a) and longitudinal section (b).

data is one of the most accurate predictor investigations. Researchers have developed an algorithm whereby the rebound value from the Schmidt hammer and the compression wave velocity from the ultrasonic test can be correlated with actual compressive strength of the concrete. The correlation of the different testing methods with actual compressive strength is commonly known as the SONREB (i.e. *SONic REBound*) method. The conducted investigation in the *Supercinema* were performed on a series of two beams and four columns and provided an average compressive strength of the concrete equal to ~23 MPa. The measures had a scatter <10%, thus no more investigations were needed since the quality of the concrete can be considered uniform in the RC structure.

2.3.3. Thermo-Camera. The area in front of the bar (see again Figures 2(c) and 2(d)) was roofed with a horizontal floor covered by a plastic-based countertop. The latter, when partially removed, allowed to point out the thermocamera. The result is shown in Figure 6. A floor connecting the masonry and RC structures emerged by the difference in temperature. It is evident the scheme of the joists (at 9–10°C) and the brick pots (at 14–16°C). This floor was joined to the structures by a simply supported lateral beams (Figure 7). Furthermore, using a laser meter, it was discovered that the soffit of the floor is at an intermediate height between the soffit of the masonry building and the soffit of the reinforced concrete building according to Figure 8.

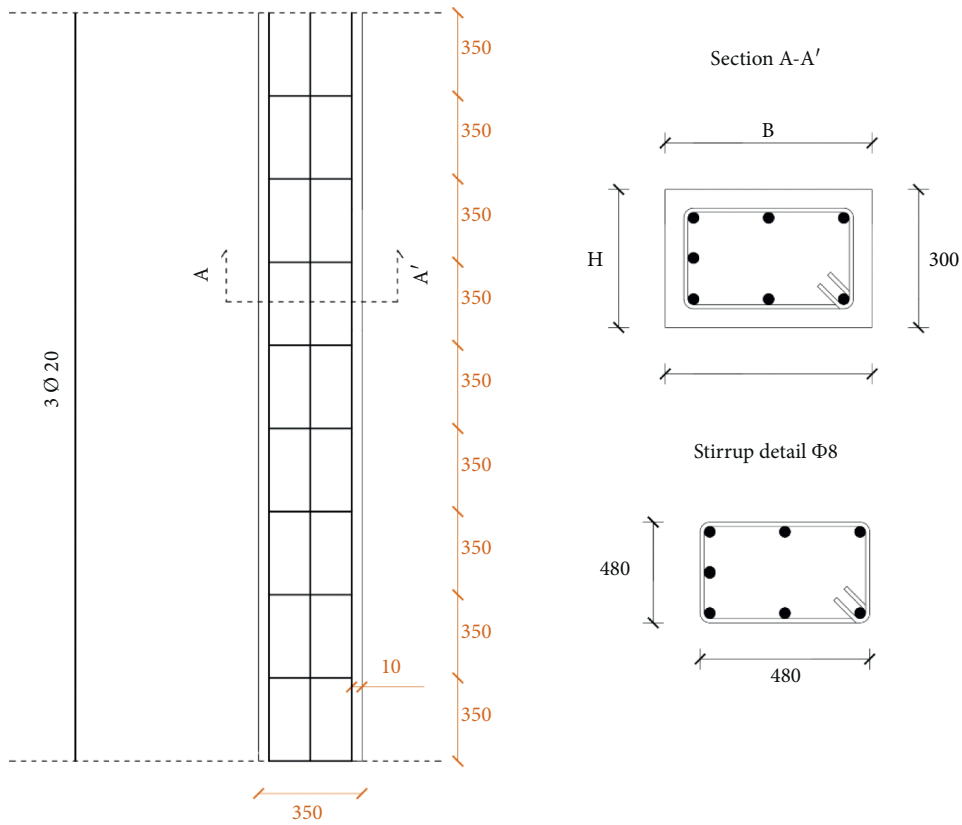

Figure 5: Identification of internal reinforcing bars of the column: cross section (a) and longitudinal section (b).

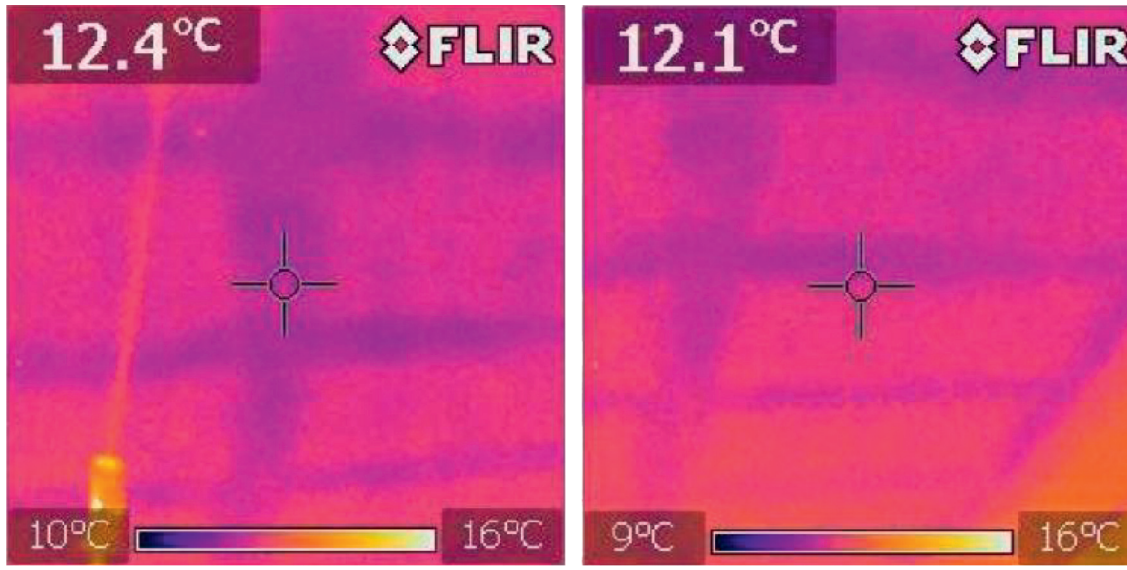

Figure 6: Thermo camera outcomes.

3. Architectural Project

The *Supercinema* is intended to be converted from a cinema-theatre to a multiplex with five projection rooms (three new) and different areas for entertainment and/or alternative service. While, the layout and functionality of the individual rooms within the masonry building are planned to be maintained unaltered according to Figure 9. So, an entrance with a box office and bar corner, the auditorium (ROOM 2), the office and a bookshop corner are prepared. On the ground floor of the reinforced concrete building, the stalls in ROOM 1 will be renovated. On the first floor (see Figure 10), the galleries to the side of the stage will be converted into an alternative use of the space with tables and chairs, while the

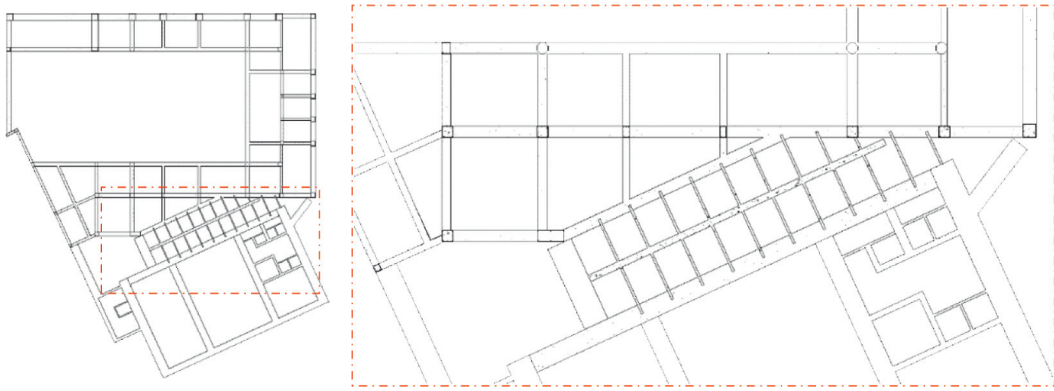

Figure 7: Detail of the connecting floor: identification (a) and zoom (b).

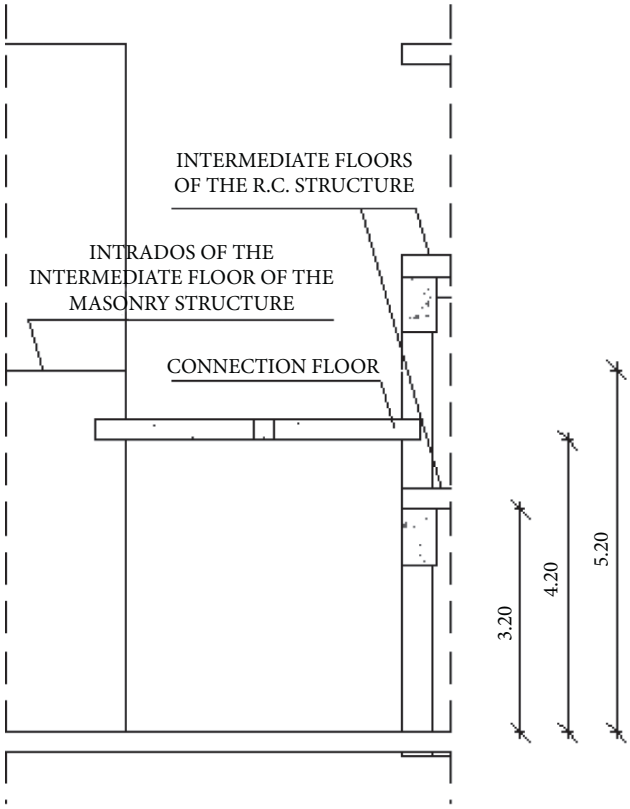

Figure 8: Transversal view of the connecting floor.

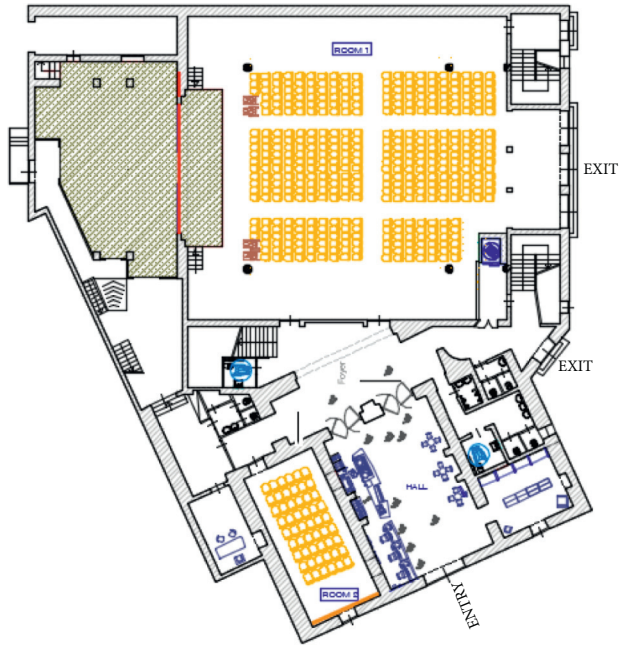

Figure 9: Ground floor layout.

one in front of the stage will remain in its original function. On the second floor, the galleries at the side of the stage will become two halls (ROOM 3 and ROOM 4) following the 1.80 m extension of the ceiling, while the one at the front will become an additional hall (ROOM 5) as shown in Figure 11. Furthermore, toilets for the disabled and lift shafts will be added. The architectural design envisages seating arrangements as follows: 54 seats for ROOM 2, 416 seats for ROOM1, 56 seats for the first-floor gallery, 58 for ROOMS 3 and 5 and 63 for ROOM 4, for a total of 705 seats. A few render views are illustrated in Figure 12 in order to give and idea of the project when completed.

Expanding the floor between the second and third decks in order to create three new halls at the current galleries means a higher load due to both crowding and the presence of seats that will act at along the almost 14 m long span of the beam which is already poorly reinforced. Therefore, in the following paragraphs, the bending behavior of the beam is studied, constrained at the ends by two simply supports in order to maximize the deflection in the middle-span cross section. Moreover, the strengthening is also simulated. In particular, the beam was studied using finite element software, i.e. MIDAS FEA NX [10], and the bending reinforced was proposed because of the Superintendence advised against the construction of a new support column at the middle span of the overloaded beam. In this scenario, the use of composite materials, i.e. carbon fiber plate (CFRP-Carbon Fiber Reinforced Polymer) installed on the intrados, is a suitable solution by taking advantage of their lightness, high mechanical strength and high resistance to corrosion. In addition, reinforcement was also studied using metal reinforcement plate on the intrados and extrados of the beam, connected by connectors.

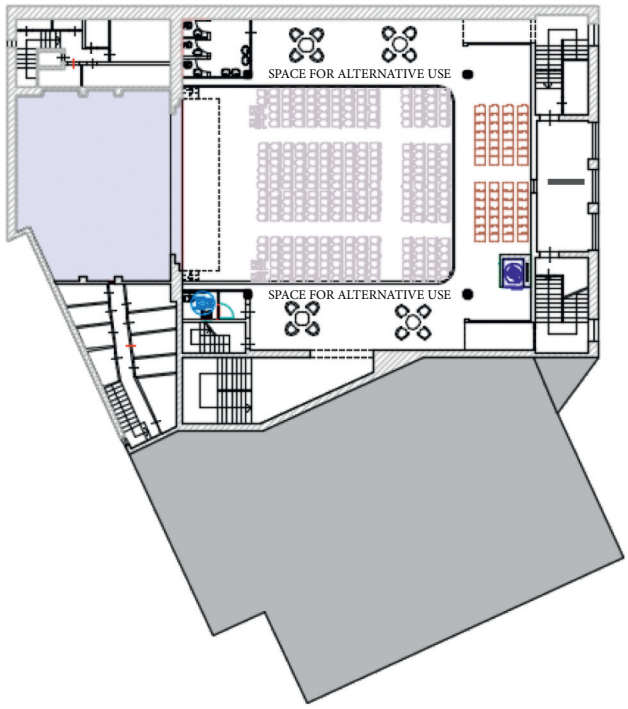

Figure 10: First floor layout.

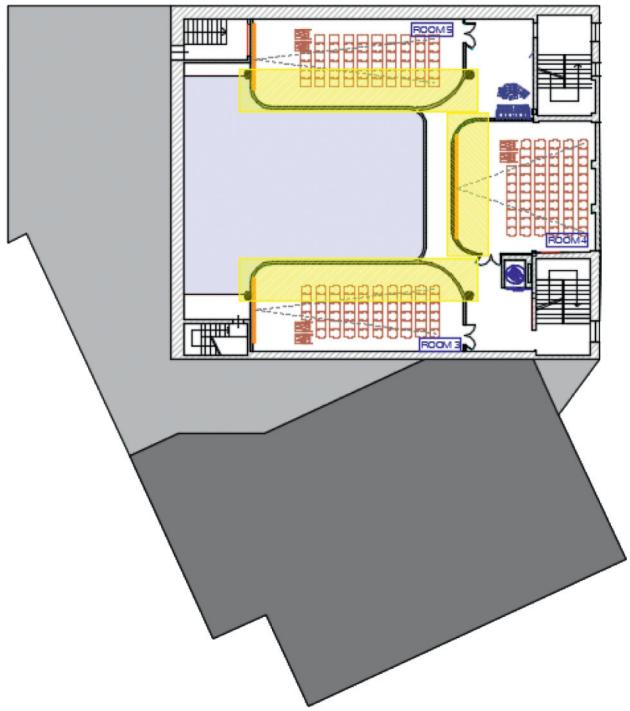

FLOOR TO BE EXTENDED

Figure 11: Second floor layout.

4. Seismic Upgrading Project

Transforming the cinema into a multiplex, changing the serviceability load of the building, does not only mean architecturally designing the arrangement of the rooms, but also possibly increasing the demand of a structural element; therefore, the bending behavior of the beam on which the floor to be extended was studied and its structural reinforcement was designed. With the help of Autodesk Revit software [11], which uses the BIM (*Building Information Modeling*) methodology, starting from the architectural model (Figure 13(a)), the structural model (Figure 13(b)) was built with the structural elements (beams and columns with their reinforcements and load-bearing walls).

Since the masonry building has not been investigated and since the two structures are made of different construction materials, a seismic joint was designed for separating the two bodies and avoids the phenomenon of hammering in the event of an earthquake. Particular attention must be focused when two buildings are placed next to each other, since in the event of seismic action they will have a different response in terms of lateral displacement depending on their mass and stiffness despite being subjected to the same ground acceleration since having a different and independent vibrating mode. Therefore, the joint must ensure an adequate reciprocal distance between two adjacent buildings, whether new or existing. This distance was foreseen in the design phase by calculating the displacements, due to seismic action, of the points of the constructions facing each other and respecting the minimum limits foreseen by the technical regulations. According to the NTC 2018, a distance between two adjacent constructions must be ensured such as to avoid hammering, which is equal to:

$$\frac{1}{100} \cdot \frac{2 \cdot a_g \cdot S}{g} \cdot h. \tag{1}$$

With:

(i) h building height;
(ii) a_g maximum horizontal acceleration at the site;
(iii) g acceleration of gravity;
(iv) S coefficient considering the subsoil category and typographical conditions, equal to: $S = S_S \cdot S_T$;
(v) S_S stratigraphic amplification coefficient;
(vi) S_T topographic amplification coefficient.

To calculate the maximum horizontal acceleration at the site, the parameters related to the site were considered as following listed down:

(i) nominal life (50 years);
(ii) class of use (III);
(iii) reference life (75 years);
(iv) spectrum (SLV 10%);
(v) probability of exceeding the reference life (10%);
(vi) return period (712 years).

The outcomes are reported in Table 1.

A minimum distance between the two buildings of 4 cm was computed. As can be seen in Figure 14, in order to separate the two buildings (red line), the load-bearing walls need to be cut (indicated by the green hatching), a 30 cm

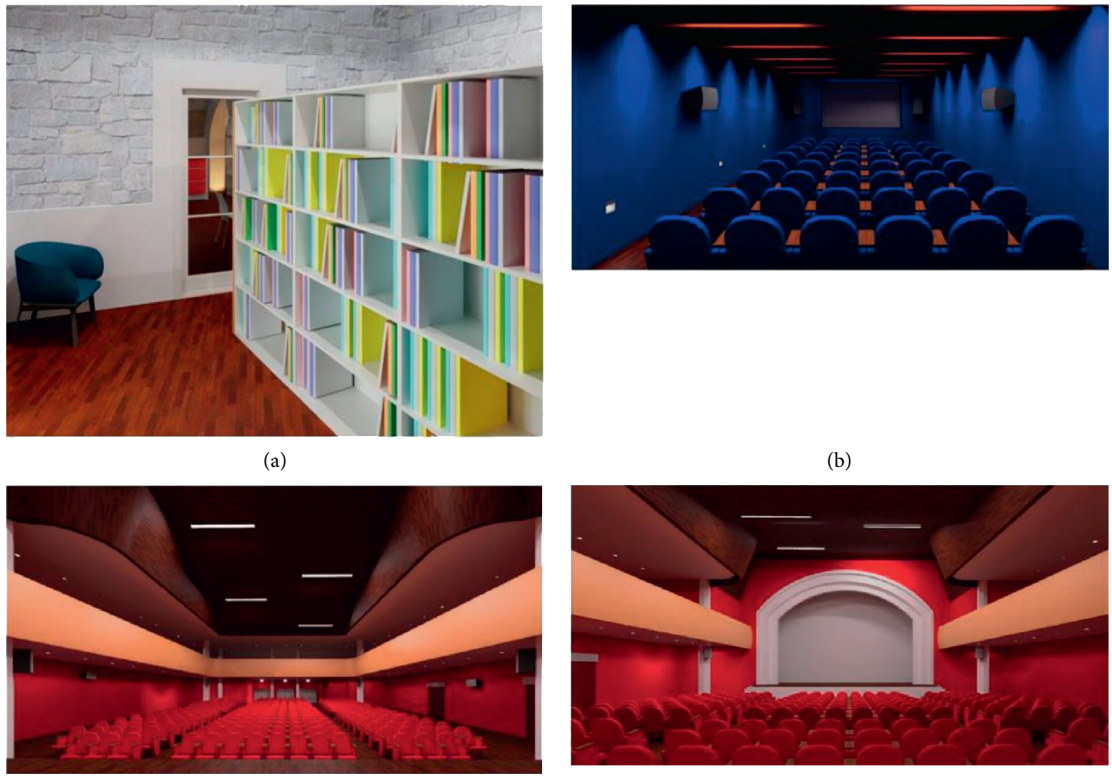

(a) (b) (c) (d)

Figure 12: Render simulation of the Supercinema: (a) recreation area, (b) ROOM2 and (c-d) ROOM1.

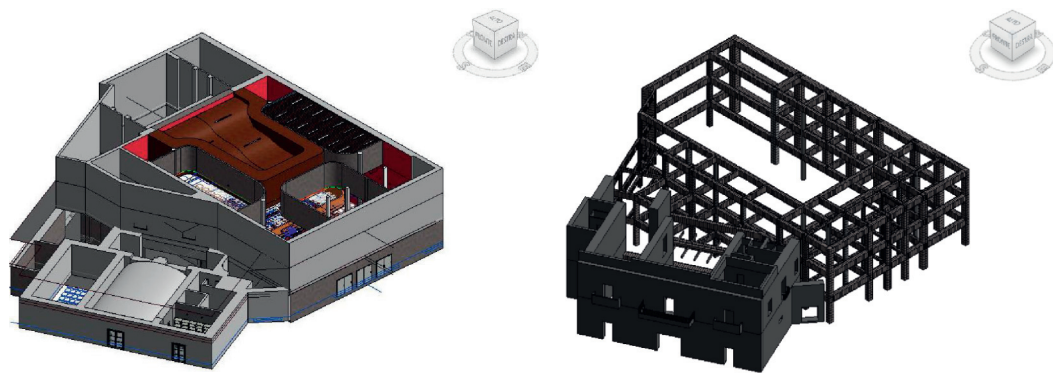

(a) (b)

Figure 13: Supercinema: (a) architecture and (b) structure evidences.

Table 1: Seismic data.

h	S_S	S_T	a_g/g	F_0	T_C
[m]	[-]	[-]	[-]	[-]	[s]
9.90	1.20	1.00	0.107	2.5	0.37

beam is created (indicated by the yellow hatching) on which the connecting floor will rest, and 3 rectangular 50×30 cm pillars and 1 trapezoidal pillar are built (indicated by the blue hatching).

The use of BIM was useful in the transition from the architectural model to the structural model in order to better understand the *skeleton* of the two structures and to be able to produce the joint in a feasible way. The global behavior of the structure was studied using the PRO_SAP [12] calculation software in order to evaluate and verify the principal stresses. Only the reinforced concrete building was modelled by inserting beams, columns and floor frames. The

Figure 14: Seismic joint location.

constrains were perfect fixed type. The model and the acting stresses represented in the Figure 15(a) and 15(b) were obtained. It is evident as the critical element is the very long span beam, which figured out the maximum bending stress (see redo color in Figure 15(b)). In particular, the value of the load acting on the beam, with the most unfavorable combination (seismic combination), is 52.89 kN/m: this value was then inserted as a uniformly distributed load on the beam span to carry out the analyses with the Midas FEA NX software.

5. Local Beam

The bending deficiency of the *very long span beam* (VLSB), about 14 m, was before mentioned. The problem is related to two main aspects: the high sustained load on the span itself ratio and the poor-quality concrete with the modest internal steel strengthening (both stirrups and longitudinal steel rebars). Therefore, the bending strengthening was focused on the *External Bonded* (EB) systems and designed by means of *Finite Element Method* (FEM). In particular the use of laminate plates was considered by comparing two different materials: carbon (CFRP - *Carbon Fiber Reinforced Polymer*) and steel (BP - *Beton Plaquè*). The numerical procedure was assessed using the commercial code MIDAS FEA NX [10]. It is in the knowledge of the authors that the majority of the RC beams tested in the laboratory have a length ranging in 3–5 m according to the literature, [13–16]. In particular, the adopted test setup is simply supported with punctual applied load (P) in almost all cases. In [17] it is possible to observe the continuous (on three supports) RC beams with an exceptional length of 8.5 meters, but the test setup adopted reported the RC beams with two bending spans of 4.25 m. In [18] it is possible to observe different boundary conditions, at one end the RC beams was clumped while at the other end a torsional constraint in order to test beams at torsion. Definitely, the literature regarding the case study presented in this work (type applied load and the entire RC beam long) is poor.

5.1. Geometrical Modelling and Boundary Conditions. The beam was three-dimensions (3D) modelled in order to replicate the entire beam in the most reliable way. Since the imposed load was full-gravitational oriented, the end constrains were simulated to be reactive only against the vertical translation. In addition, one of the ends constrains was also set to avoid the horizontal translation in the perspective of numerically consider an isostatic structural member. However, the considered beam was a continuous element simply supported by many columns (more than two), the static schema was assumed to be the uniformly distributed load on two simply supports, in order to emphasize the deflection in the middle of the beam given the high span of about 14.0 m. It is felt by the authors that the choice is consistent with the real case study since the critical span was highly longer than the others while the overloading is acting only on it. Moreover, the limited number of the internal rebars, associated to their level of corrosion, are both factors indicating that a rotation at the ends of the VLSB is potentially reliable and, anyway, on the conservative side. The geometry and the internal reinforcement are both illustrated in Figure 4. This modelling technique, find in literature [19–26], is useful for establishing the real behavior and the complete crack pattern along the entire beam. The technical literature is rich of case studies where the FE technique is used to study the behavior of the entire structure or individual members [27–35]. The herein considered beam was modelled using a structured mesh with tetrahedral type elements. The characteristic element length equal to 10 mm was evaluated through the relationship provided by Midas [10]. The internal reinforcement was modelled through a linear truss, while the external reinforcement was modelled by a shell element with linear interpolation functions. Finally, a perfect bond was assumed both between the beam and external reinforcement and the concrete and internal reinforcement. In Figure 16, a 3D FE mesh was reported. In particular, the adhesion between the concrete and the reinforcing rebars was defined through the internal function called embedded regions. The embedded technique is used to specify that the internal reinforcement is embedded in host elements (beam).

5.2. Materials Model. The concrete smeared cracking function was used to model the two principal concrete failure mechanisms such as the tensile cracking and the compressive crushing. This model is designed for the applications in which the concrete is subjected to essentially monotonic loading and it uses oriented damaged elasticity concepts (smeared cracking) to describe the reversible part of the material's response after cracking failure. The constitutive compressive law of concrete was modelled by nonlinear relationship proposed by *Thoronfeldt et al.* [36], where f_c and ε_c are the compressive strength and relative strain. The descending branch is possible to define it through a

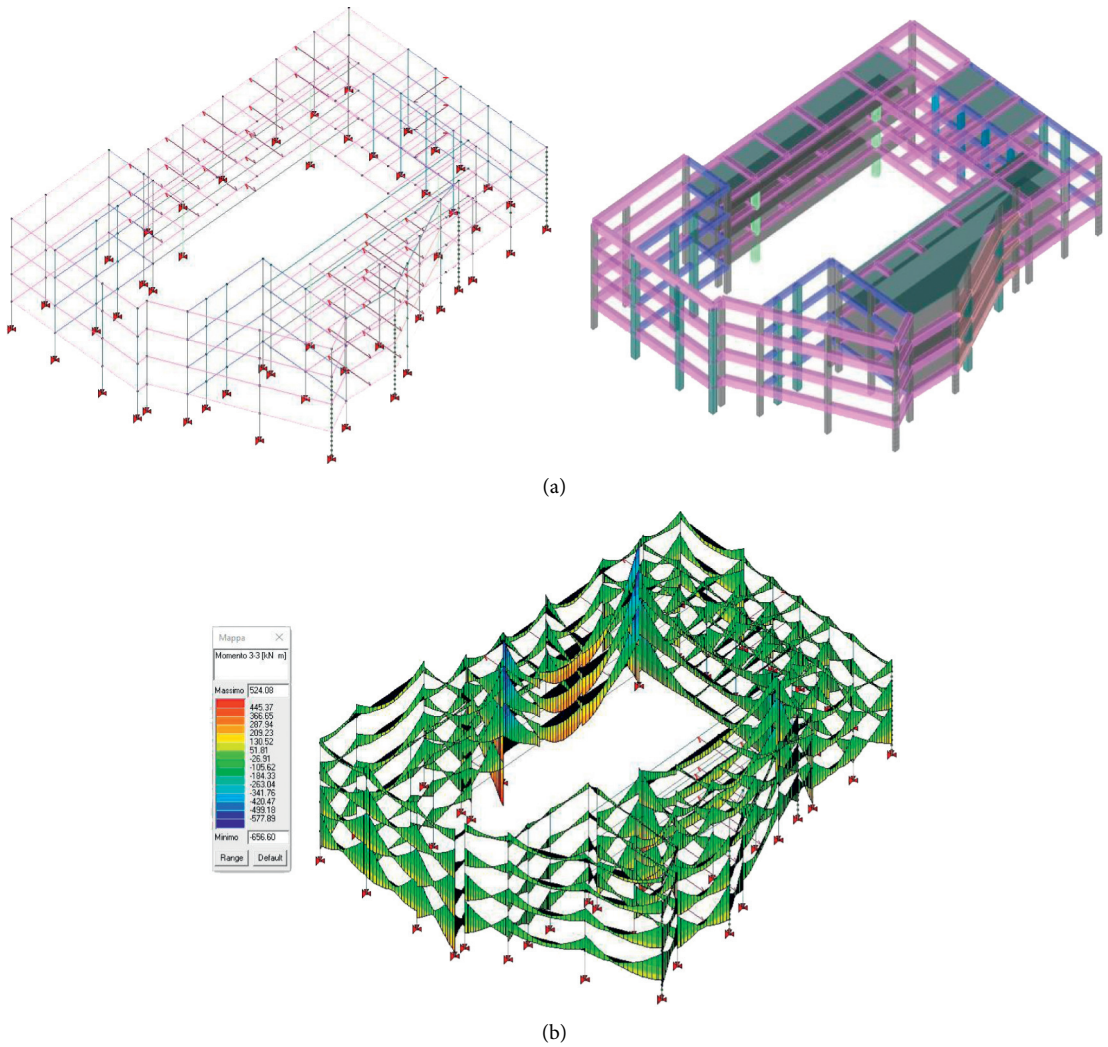

Figure 15: RC-structure global model in seismic load combination without any strengthening: (a) beam and 3D model and (b) results.

coefficient k, as reported in [36]. The constitutive tensile law was modelled by the relationship proposed by Hordijk, [37]. The model's parameters used are the tensile strength $f_t = 1.59$ MPa, the fracture energy $G_f = 0.08$ N/mm. In Figure 17 the materials constitutive laws were reported.

The steel constitutive law used to model the longitudinal steel and the stirrups was considered by means of elastic-plastic hardening trend, both in tension and compression. In the linear elastic range, the behavior has been defined by the density ($\rho = 7.85$ g/cm^3), *Young's modulus* ($E_s = 210$ GPa) and Poisson's ratio ($v = 0.3$). Instead, the plastic-hardening branch has been defined through the yield strength (equal to356 MPa), the ultimate strength (equal to 856 MPa) and the deformation values corresponding to the two strengths considered. The investigated beam was reinforced with two reinforcement systems CFRP and BP. Both systems were modelled as a homogenous material by a shell element with the linear interpolation functions. Therefore, the constitutive tensile laws were linear elastic until failure for the CFRP system, while linear elastic until the yield stress and then perfect plastic for BP-system. The input data parameters are modulus (E_f), thickness (t), yield stress (f_y) and the ultimate strain (ε_u) and they were summarized in Table 2. In addition, the CFRP system has been applied on a part of the beam width equal to 15 cm in the tension zone, while the BP system was applied on the whole beam width. In particular, the external reinforcement was applied both in the flexural compression and tensile side of the existing beam. The two steel plates, in the numerical model was not connected. The selected reinforcement systems are BP and CFRP. Both systems have the drawback of employing skilled workers. The CFRP system presents a thickness of just over 1 mm and its installation is easy and fast. The main advantage consists of the not sensitivity to the corrosion differently to the steel. The disadvantage of CFRP is that it has linear elastic until the rapture behavior which means poor ductility. Furthermore, it is sensible to high temperature. The BP system has greater resistance to high temperatures and has non-linear behavior. The disadvantages are the thicknesses and installation time of the reinforcement.

5.3. Numerical Results. The analysis was conducted under enforcing displacements–λu in y-directions and the non-linear equations were solved by the well-known *Newton's*

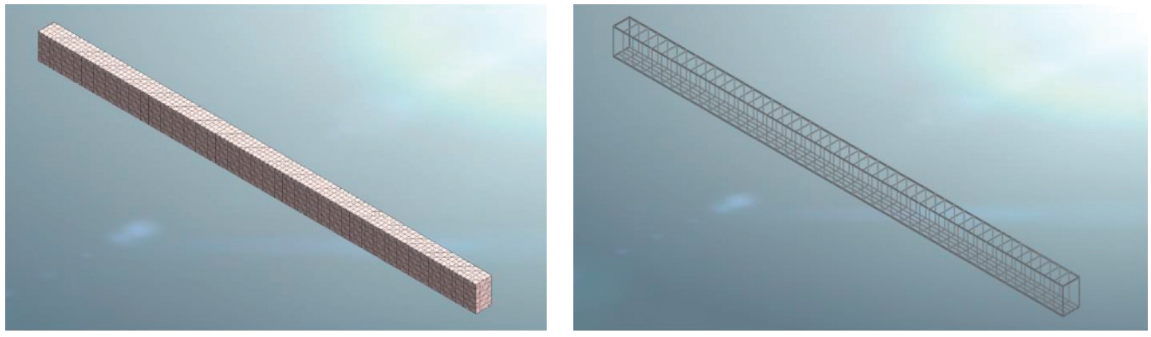

(a) (b)

Figure 16: Geometrical modelling and FE resolution: (a) concrete and (b) internal reinforcement.

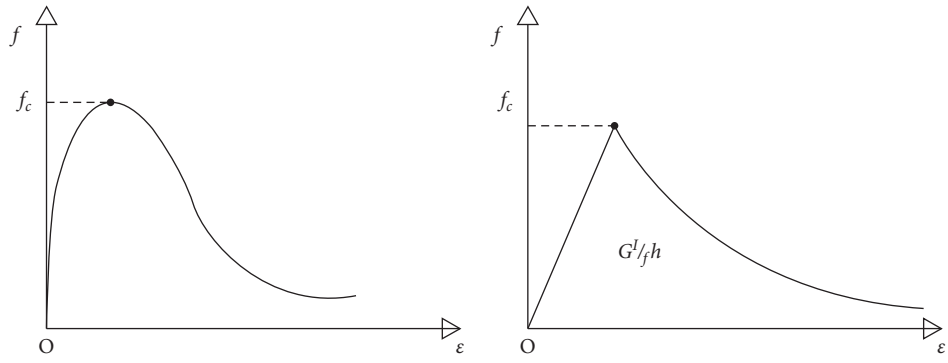

(a) (b)

Figure 17: Material constitutive laws: (a) compression and (b) tension.

Table 2: Parameters for the EBs.

External reinforcement	E [GPa]	t [mm]	f_y [MPa]	ε_u [%]
CFRP plate	170	1.4	—	1
BP	210	5	275	2

modified method. The aim is to recompute the global stuffiness of the structure at each load step. Consequently, the method is costly from the computational point of view in the n-step while faster at global level. Moreover, the Newton's modified method for determining a root of a nonlinear equation $f(x) = 0$ has long been favored for its simplicity and fast rate of convergence. *Newton's modified method* iteratively produces a sequence of approximation that converge quadratically to a simple root. While a few rules with higher order convergence have long been known, these have the disadvantage of requiring higher order derivatives.

Figure 18 shows the numerical curves in terms of applied total load versus mid-span section deflection. In addition, the dashed lines indicate the load value to which the existing beam is currently subjected, which is equal to 224 kN (green line), and the load to which it will be subjected after the change of serviceability of the building and, at the same time, the extension of the floor (see Section "Architectural project") or rather equal to 589 kN (orange line).

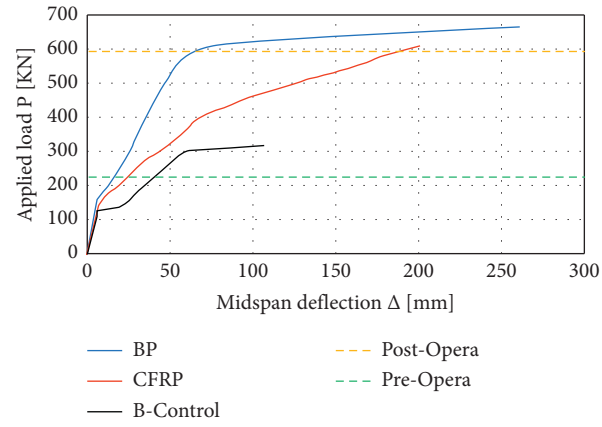

Figure 18: Load vs deflection law: comparison of the results.

First of all, from Figure 18 it can be seen that the actual capacity of the beam (black line) is largely major of the potential original design load (i.e. 224 kN), while it is dramatically minor when compared with the demand reached after the multiplex conversion (i.e. 589 kN). The red and blue numerical curves represent the reinforcement scenario of the existing beam with CFRP and BP, respectively. Both the reinforcement systems resulted, in terms of applied load, to

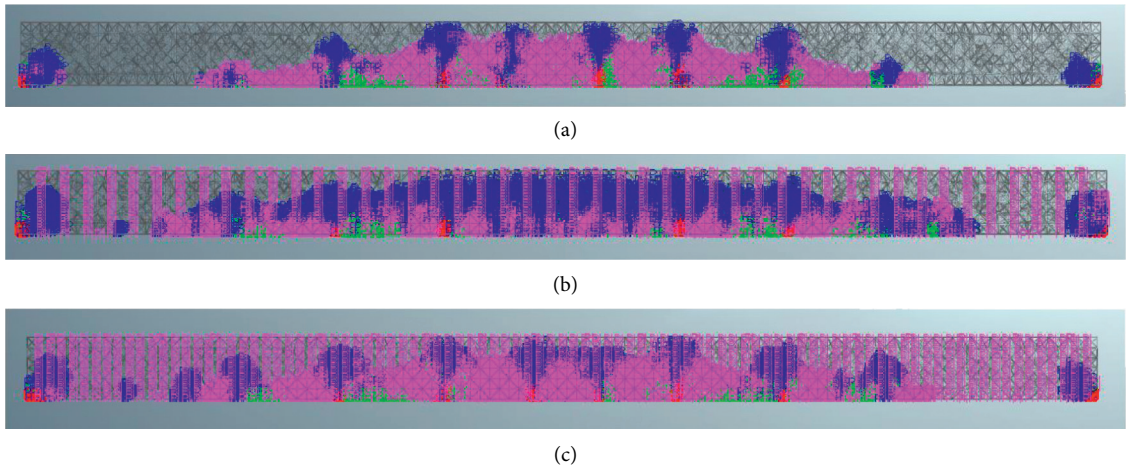

(a)

(b)

(c)

Figure 19: Crack pattern when the first crack opening: (a) B-Control, (b) CFRP and (c) BP.

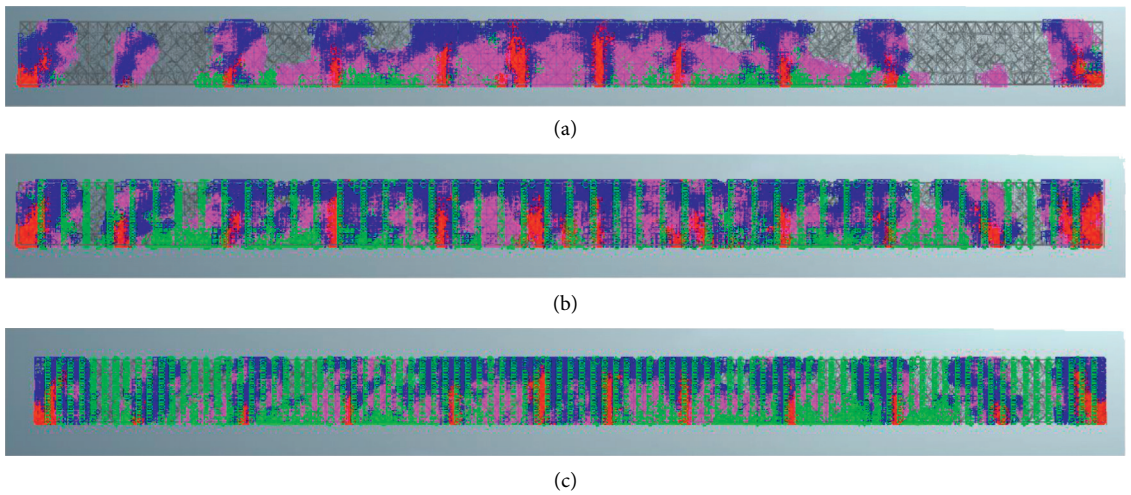

(a)

(b)

(c)

Figure 20: Crack pattern at ultimate limit state: (a) B-Control, (b) CFRP and (c) BP.

have greater load bearing capacity if in contrast with the required limit load, again 589 kN. On the other hand, the bending capacity expressed in terms of deflection is a further crucial aspect. In fact, the CFRP solution exhibited a larger deformation (i.e. 200 mm) at the mid-span level when compared with the BP alternative before the yielding (i.e. 61.44 mm). nonetheless, in both cases the deflection is relatively low if normalized per the span of the beam providing an optimal solution in order to take into consideration of the limitations in the Italian standard [8]. Furthermore, the stiffness in the elastic range is considerably higher for BP instead of CFRP. Moreover, according to Figure 18, the reinforcement called BP satisfied the mechanical performance required of the structure post-opera. The adopted solution affords the reinforced element an increase in terms of initial stiffness if compared with the other solution. Moreover, the BP reinforcement system in terms of midspan deflection after the yield point shows an applied load response curve with a plateau very emphasized. This solution presents a disadvantage in terms of added thickness (see Table 2) in comparison with the CFRP reinforcement technique. The reliability of the proposed FE model is testified also by the evaluation of the failure modes. At this scope the comparison of the crack patterns at the first crack opening step and at the ultimate limit state condition are illustrated in Figures 19 and 20, respectively. As expected, the first crack (in red) opens at mid-span level and the next one trend to have constant distance each other in between two consecutive stirrups. By observing the ultimate state, the development of the cracks (again in red) is more evident with a pseudo vertical trend. It is also noticeable that the number of cracks is almost the same in all the configurations.

6. Conclusions

The case study herein presented report on the common problem of overloading and seismic deficiency due to the chance of serviceability of a cultural Heritage: the *Supercinema* in *Trani* (Italy). The study dealt with a scientific key, or rather the aid of advanced tools for surveying, analyzing and verifying the structures. In order to be able to carry out the three new projecting rooms in correspondence with the

current galleries on the second floor, it was decided to design the attic between the second and third deck. In these new rooms, the overloading was fully located on an approximately 14 m long span RC-beam.

Before proceeding with the study and reinforcement of the beam, since the building is composed of two adjacent structures of different construction system, the structural model was first developed, starting from the architectural model, thanks to the help of the Autodesk Revit BIM software that allowed to better understand the position of the structural elements. Subsequently, a seismic structural joint was designed in order to "separate" the two structures.

Secondly, modelling the beam within the Midas FEA NX finite element software was performed aiming to simulate the bending strengthening by means of both CFRP-plate (CFRP) and *Beton Plaquè* (BP), in a non-linear static analysis. The results demonstrated the effectiveness of the two proposed solutions in terms of both loads bearing capacity (almost doubled) and mid-span deflection (ranging between two and three times more). It was found the steel strengthening is the most suitable for the intervention since it is significantly stiffer.

Data Availability

all data are avaiable on request.

Conflicts of Interest

The authors declare to have not conflicts of interest.

Acknowledgments

The authors would like to sincerely thank the owners of the building for having guaranteed access and the possibility to investigate and study the structure.

References

[1] ICOMOS/Iscarsah Committee, "Recommendations for the Analysis, Conservation and Structural Restoration of Architectural Heritage," 2005, http://www.icomos.org.

[2] A. Formisano, A. Massimilla, G. Di Lorenzo, and R. Landolfo, "Seismic retrofit of gravity load designed RC buildings using external steel concentric bracing systems," *Engineering Failure Analysis*, vol. 111, Article ID 104485, 2020.

[3] M. D'Amato, A. Gigliotti, and R. Laguardia, "Seismic isolation for protecting historical buildings: a case study," *Frontiers in Built Environment*, vol. 5, no. 87, 2019.

[4] A. Miano, G. Chiumiento, A. Formisano, and A. Prota, "Influence of different knowledge levels on the seismic retrofit cost assessment of a RC school building," in *AIP Conference Proceedings,* vol. 2293, no. 1, AIP Publishing LLC, Article ID 380014, 2020.

[5] M. Laterza, M. D'Amato, and R. Gigliotti, "Modeling of gravity-designed RC sub-assemblages subjected to lateral loads," *Engineering Structures*, vol. 130, pp. 242–260, 2017.

[6] R. J. Williams, P. Gardoni, and J. M. Bracci, "Decision analysis for seismic retrofit of structures," *Structural Safety*, vol. 31, no. 2, pp. 188–196, 2009.

[7] N. Berlucchi and S. Cicognetti, "Restauro e adeguamento normativo di un teatro all'italiana: il Sociale di Camogli," *Restauro e adeguamento normativo di un teatro all'italiana: il Sociale di Camogli*, vol. 9, pp. 27–42, 2020.

[8] Ntc 2018, *Ntc 2018 – Nuove Norme Sismiche Per Il Calcolo Strutturale*, 2018.

[9] Circolare, *Istruzioni per l'applicazione dell'«Aggiornamento delle "Norme tecniche per le costruzioni"» di cui al decreto ministeriale 17 gennaio 2018*, 2019.

[10] F. E. A. Midas, *Advanced Nonlinear and Detail Program, Analysis and Algorithm*, 1989.

[11] L. Khemlani, *Autodesk Revit: Implementation in Practice*, 2004.

[12] PROfessional Structural Analysis Program, "PROfessional Structural Analysis Program," 2020, https://www.2si.it/it/.

[13] A. Balsamo, F. Nardone, I. Iovinella, F. Ceroni, and M. Pecce, "Flexural strengthening of concrete beams with EB-FRP, SRP and SRCM: experimental investigation," *Composites Part B: Engineering*, vol. 46, pp. 91–101, 2013.

[14] O. Rosenboom and S. Rizkalla, "Modeling of IC debonding of FRP-strengthened concrete flexural members," *Journal of Composites for Construction*, vol. 12, no. 2, pp. 168–179, 2008.

[15] M. A. Aiello, M. Leone, and L. Ombres, "Structural analysis of reinforced concrete beams strengthened with externally bonded FRP (fiber reinforced polymers) sheets," in *Proceedings of the Third International Conference on "composites in Constructions"*, pp. 11–18, Lyon, France, July, 2005.

[16] L. Ombres, "Flexural analysis of reinforced concrete beams strengthened with a cement based high strength composite material," *Composite Structures*, vol. 94, no. 1, pp. 143–155, 2011.

[17] A. F. Ashour, S. A. El-Refaie, and S. W. Garrity, "Flexural strengthening of RC continuous beams using CFRP laminates," *Cement and Concrete Composites*, vol. 26, no. 7, pp. 765–775, 2004.

[18] M. Y. Alabdulhady, L. H. Sneed, and C. Carloni, "Torsional behavior of RC beams strengthened with PBO-FRCM composite-an experimental study," *Engineering Structures*, vol. 136, pp. 393–405, 2017.

[19] L. Ombres and S. Verre, "Experimental and numerical investigation on the steel reinforced grout (srg) composite-to-concrete bond," *Journal of Composites Science*, vol. 4, no. 4, p. 182, 2020.

[20] F. Bencardino, M. Nisticò, and S. Verre, "Experimental investigation and numerical analysis of bond behavior in SRG-strengthened masonry prisms using UHTSS and stainless-steel fibers," *Fibers*, vol. 8, no. 2, p. 8, 2020.

[21] L. Ombres and S. Verre, "Numerical modeling approaches of FRCMs/SRG confined masonry columns," *Frontiers in Built Environment*, vol. 5, p. 5, 2019.

[22] L. Ombres and S. Verre, "Flexural strengthening of RC beams with steel-reinforced grout: experimental and numerical investigation," *Journal of Composites for Construction*, vol. 23, no. 5, 2019.

[23] S. Verre, "Three-dimensional numerical modeling of RC beam strengthened in shear with steel reinforced grout (SRG)," in *Proceedings of the 1st Fib Italy YMG Symposium on Concrete and Concrete Structures*, pp. 64–71, Krakow, Poland, May, 2019.

[24] L. Ombres and S. Verre, "Numerical analysis of the structural response of masonry columns confined with SRG (steel reinforced grout)," *MetroArchaeo*, vol. 2017, pp. 718–722, 2019.

[25] S. Verre, A. Cascardi, M. A. Aiello, and L. Ombres, "Numerical Modelling of FRCMs Confined Masonry Column," *Key Engineering Materials*, vol. 817, 2019.

[26] L. Ombres and S. Verre, "Masonry columns strengthened with steel fabric reinforced cementitious matrix (S-FRCM) jackets: experimental and numerical analysis," *Measurement*, vol. 127, pp. 238–245, 2018.
[27] H. Pirsaheb, P. Wang, M. Javad Moradi, and G. Milani, "A Multi-Pier-Macro MPM method for the progressive failure analysis of perforated masonry walls in-plane loaded," *Engineering Failure Analysis*, vol. 127, Article ID 105528, 2021.
[28] A. Ferrante, E. Giordano, F. Clementi, G. Milani, and A. Formisano, "FE vs. DE modeling for the nonlinear dynamics of a historic church in Central Italy," *Geosciences*, vol. 11, no. 5, p. 189, 2021.
[29] F. Clementi, "Failure analysis of apennine masonry churches severely damaged during the 2016 central Italy seismic sequence," *Buildings*, vol. 11, no. 2, p. 58, 2021.
[30] A. Ferrante, M. Schiavoni, F. Bianconi, G. Milani, and F. Clementi, "Influence of stereotomy on discrete approaches applied to an ancient church in Muccia, Italy," *Journal of Engineering Mechanics*, vol. 147, no. 11, Article ID 04021103, 2021.
[31] M. Valente, "Seismic vulnerability assessment and earthquake response of slender historical masonry bell towers in South-East Lombardia," *Engineering Failure Analysis*, vol. 129, Article ID 105656, 2021.
[32] V. Sarhosis, D. Dais, E. Smyrou, İ. E. Bal, and A. Drougkas, "Quantification of damage evolution in masonry walls subjected to induced seismicity," *Engineering Structures*, vol. 243, Article ID 112529, 2021.
[33] A. Ferrante, D. Loverdos, F. Clementi et al., "Discontinuous approaches for nonlinear dynamic analyses of an ancient masonry tower," *Engineering Structures*, vol. 230, Article ID 111626, 2021.
[34] A. Kita, N. Cavalagli, M. G. Masciotta, P. B. Lourenço, and F. Ubertini, "Rapid post-earthquake damage localization and quantification in masonry structures through multidimensional non-linear seismic IDA," *Engineering Structures*, vol. 219, Article ID 110841, 2020.
[35] N. Grillanda, L. Cantini, L. Barazzetti, G. Milani, and S. Della Torre, "Advanced modeling of a historical masonry umbrella vault: settlement analysis and crack tracking via adaptive NURBS kinematic analysis," *Journal of Engineering Mechanics*, vol. 147, no. 11, Article ID 04021095, 2021.
[36] E. Thorenfeldt, A. Tomaszewicz, and J. J. Jensen, "Mechanical properties of highstrength concrete and applications in design," in *Proceedings of the Symp. Utilization of High-Strength Concrete (Stavanger, Norway)*, Trondheim, Norway, January, 1987.
[37] D. A. Hordijk, "Local Approach to Fatigue of Concrete," PhD Thesis, Delft University of Technology, Delft, Netherlands, 1991.